CycleGANWM: A CycleGAN watermarking method for ownership verification

Dongdong Lin, Benedetta Tondi, Bin Li, Mauro Barni

***Abstract*—Due to the proliferation and widespread use of deep neural networks (DNN), their Intellectual Property Rights (IPR) protection has become increasingly important. This paper presents a novel model watermarking method for an unsupervised image-to-image translation (I2IT) networks, named CycleGAN, which leverage the image translation visual quality and watermark embedding. In this method, a watermark decoder is trained initially. Then the decoder is frozen and used to extract the watermark bits when training the CycleGAN watermarking model. The CycleGAN watermarking (CycleGANWM) is trained with specific loss functions and optimized to get a good performance on both I2IT task and watermark embedding. For watermark verification, this work uses statistical significance test to identify the ownership of the model from the extract watermark bits. We evaluate the robustness of the model against image post-processing and improve it by fine-tuning the model with adding data augmentation on the output images before extracting the watermark bits. We also carry out surrogate model attack under black-box access of the model. The experimental results prove that the proposed method is effective and robust to some image post-processing, and it is able to resist surrogate model attack.**

***Index Terms*—GAN watermarking, Model watermarking, CycleGAN, Intellectual property rights protection**

I. Introduction

II. Related works

As we said, in this paper, we focus on the watermarking of unsupervised image-to-image translation models. Such models are used whenever gathering a large dataset of paired images belonging to the input and output domains is impossible or too expensive. In this section, we briefly review the main architectures for unpaired image-to-image translation and the methods proposed so far to watermark image translation models, showing that such methods are not suitable for the watermarking of models containing training cycles, with particular attention to CycleGAN.

A. Unsupervised Image-to-image translation

In recent years, I2IT has become a popular topic in deep learning, and several outstanding achievements have been reached. In early works, like pix2pix [1], image pairs belonging to the input and output domains were used to train the translation network in a supervised way. In a more flexible way, unsupervised I2IT requires only that sample images from the two domains are available to instruct the network the distinguishing features of the two domains, without the need to show how each single image in the training set should be transformed.

CycleGAN [2] is the prototypical network for unpaired I2IT. The unavailability of paired images belonging to the input and output domains, is got around by including a cycle loss ensuring that when an image is brought from the input to the output domain and back, the image we get is similar to the original one. An identity loss is also introduced requiring that when an image of the output domain is fed at the input of the network, no image transformation is actually applied. CycleGAN is widely applied in many fields. For example, it successfully translates MRI to CT images and leads to mis-diagnosis of the doctor [3]. Auxiliary data like coronavirus (COVID-19) X-ray or CT images can be generated by CyleGAN then used for training a automatically detection model [4].

Several variations of the basic CycleGAN architecture have been proposed. In [5], the authors propose two pyramids of generators and discriminators trained with only two unpaired images. The input image is sampled into N scales and each scale has the same structure as CycleGAN. The generators take the downsampled input image and the preciously translated image to generate new image. Note that the first scale takes the original input image. It can achieve better performance than CycleGAN in the task of photo to painting, photo to sketch, etc. Similar works such as DualGAN [6] and DiscoGAN [7] are proposed based the cyclic loss. Unlike CycleGAN, which uses LSGAN [8] as the generator, DualGAN uses WGAN [9] as the generator, and DiscoGAN uses simple conv-deconv layers as the generator. They all contain three loss functions where CycleGAN and DualGAN use the mean absolute error (MAE) as the cycle-consistency loss but DiscoGAN uses mean square error (MSE) as the cycle-consistency loss. DualGAN confirms that the importance of the cycle-consistency loss and DiscoGAN witnesses the performance of the cyclic structure GAN on different tasks like photo to sketch, label to photo and gender change.

In multi-domain translation task, AsymGAN [10] applies cycle-consistency loss on three color channels of RGB separately and uses the one-hot label which based on StarGAN [11], to differentiate multi domains. It achieves better visual performance of the translation than StarGAN.

In [12] an attention module is introduced to help the network focusing on the most relevant parts of the input image to improve image transfer from selfie to anime images [13].

Finally, the authors of [14], introduce a constraint in the shared-latent space to modify the attributes of face images.

D. Lin was with College of Electronic and Information Engineering, Shenzhen University, Shenzhen 518060, China. E-mail: dongdonglin8@gmail.com

B. Generative adversarial network IPR protection

Watermarking of generative models is usually achieved in a black-box or no-box modality [15]. Though the GAN model acts as the watermark carrier, the watermark is retrieved from the output images produced by the model, either in correspondence to specific inputs (black-box watermarking), or from any image generated by the model regardless of the image used as input (no-box watermarking),.

In [16] the authors propose a black-box GAN watermarking method producing output images containing a visible watermark, when the network is fed with specific triggering images, e.g., an image containing a small noisy area. This method works for a variety of networks, including generative networks, image transfer networks and super-resolution networks.

In [17], [18], the authors show that it is possible to watermark a GAN network by simply training the network on watermarked images. As a first step, they have trained an image watermarking network and a decoder network, which are a slightly modified version of StegaStamp [19] networks. After training, the watermarking network learns to embed a visible watermark into the inout image. The images obtained in this way are used to watermark the images of the output domain to be used for training the I2IT network. In this way the network learns to generate images containing the watermark, since all the images in the output domain training set contain the watermark. In the watermark verification phase, the pre-trained decoder is used to extract watermark bits from the output images generated by the watermarked model, in a typical no-box watermarking setting. The above method is further improved in [20] by adding an image processing step during the training of the watermark encoder and decoder, thus achieving moderate robustness against image post-processing.

A variation of the method described in [17], [18] has been proposed by Fei *et. al.* [21]. Rather than relying on the capability of the GAN to imitate the watermarked images produced by Stegastamp shown during training, a specific step is introduced during the training phase requiring that the application of the watermark decoder to the images generated by the network results in the extraction of the correct sequence of bits. In this way a better watermark retrieval accuracy is obtained with respect to [17], [18].

A similar approach is used in [22] to embed an image logo as watermark. The main difference with respect to [21] is that the watermark decoder is trained together with the GAN rather than being pre-trained and frozen during a previous training round. An additional contribution of [22] is the introduction of an adversarial training stage to combat surrogate model attacks. Specifically, they train a surrogate model with the watermark dataset which is accessed in a black-box scenario from the GAN model, and then use the output from the surrogate model to fine-tune the watermark decoder and enhance its ability to resist the attack. A similar GAN watermarking method is proposed in [23].

Rather than decode the watermark from the output of GAN directly, the method of [23] uses a decoder to decode the watermark from the concatenation of the encoded output from an image encoder and a key encoder. The image encoder receives the output of GAN and the key encoder receives a binary secret key. The encoder, decoder and the GAN are trained together. Finally, they can verify the ownership with the decoder from the output of GAN and, more importantly, from a correct secret key.

The existing methods have witnessed the successful applications of GAN model watermarking. However, from our analysis we know that the methods proposed so far cannot applied to CycleGAN and models derived from CycleGANs, because with only the cyclic input and identity input (option) in CycleGAN can erase the watermark from embedding. Besides, there is no box-free methods applied on CycleGAN watermarking. While black-box methods, like for instance [16] could be applied to CycleGAN as well, the method [16] is proposed with visible watermark and restrict its application in real world. For invisible CycleGAN watermarking leaves a blank of research. Furthermore, a clear analysis of the way the watermark can be used for ownership verification is usually missing. Therefore, our work of CycleGAN watermarking fills these gaps and extend the research for GAN watermarking.

III. Threat model and requirements

In this section, we introduce the threat model and the ownership verification protocol wherein the proposed CycleGAN watermarking method is going to be used. Then we list the requirements that the watermark must satisfy to be successfully used within the model identified previously.

The threat model is summarised in Figure 1. We assume that the watermark owner (say Bob), after training the CycleGAN, makes it available through an API service. By accessing the API, users can transform images from an input domain $\mathcal{A}$ to an output domain $\mathcal{B}$, and viceversa. Suppose a malicious user (say Eve) wants to train her own image translation network, and suppose she wants to adopt a supervised architecture. To do so, she needs a large dataset of paired images belonging to the domains $\mathcal{A}$ and $\mathcal{B}$. To avoid the burden of gathering such paired images, Eve launches a surrogate model attack and queries the API of Bob's network to build the training dataset she needs. After training, Eve makes her model available through a remote service thus competing with Bob's service.

Due to the presence of the watermark within Bob's model, Bob, or an independent verification authority (say Alice), can query Eve's model and verify the presence of Bob's watermark thus proving that Eve's model was derived from Bob's network (Figure 1). Alternatively, Bob can inspect the images produced by Eve and still understand that they have been generated by a network derived from the watermarked one[1]. Note that Eve may apply some post-processing to the images generated by the surrogate network before distributing them to hinder the extraction of the watermark.

From the threat model we can derive the requirements of the watermark must satisfy as follows:

- *Invisibility*. Obviously the watermark should not degrade the quality of the generated images and the watermark should be imperceptible.

[1]This latter scenario may model a situation wherein Eve does not make the surrogate model publicly available but uses it to generate synthetic images and spread them over the internet.

- *Accuracy*. Detection should guarantee a good correct detection rate for a sufficiently low false positive rate
- *Robustness*. From the threat model we know that the watermark must survive from the surrogate model attack and image-post processing.
- *Payload*. A multi-bit model watermarking scheme must ensure that the host target model conveys as much information as possible. In principle a multi-bit model watermarking scheme can always transform to a zero-bit model watermarking scheme, assuming the payload is large enough. For sake of flexibility we opted for multi-bit watermarking.

In fact, a cyclic structure can definitely affect the watermark embedding since one generator's output will be fed as input of another generator and the watermark may be covered. Therefore in this paper we consider to watermark the CycleGAN, then go further to encourage and fill the blank of the research of cyclic GAN watermarking. **MB**: This concept was already discussed in the Introduction and Section II, so you do not need to repeat it here.

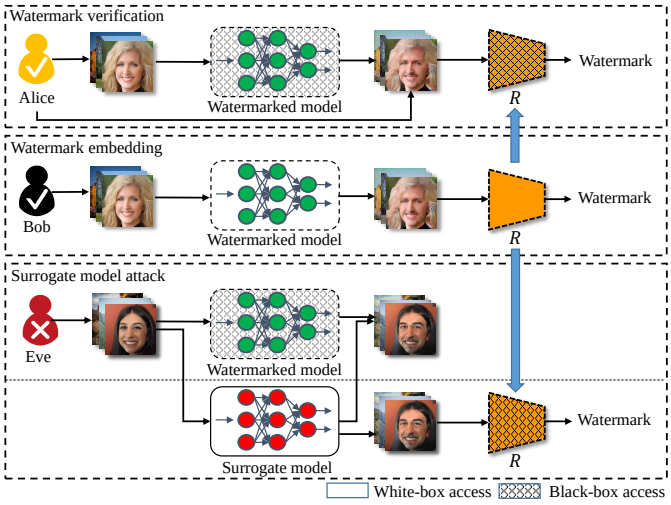

Fig. 1. The overall procedure of GAN watermarking, including watermark embedding, watermark verification and the threat model that GAN watermarking may be faced.

IV. Proposed Method

In this section, we introduce our method for CycleGAN watermarking and watermark verification. We start by detailing the CycleGAN architecture we are going to watermark, then we present out watermarking algorithm. Finally, we cast the verification protocol into an hypothesis testing framework to be used later to assess the accuracy of the watermark verification procedure.

A. CycleGAN network

Mathematically speaking, the task of CycleGAN is to learn two mapping functions G_A and G_B between two domains $\mathcal{A}$ and $\mathcal{B}$ with the given training samples $\{A_i\}_{i=1}^{M}$ where $A_i \in \mathcal{A}$ and $\{B_j\}_{j=1}^{N}$ where $B_j \in \mathcal{B}$. Two discriminators D_A and D_B are used to distinguish the generators' output images are real or fake. With adversarial training, the discriminators will force the generators generate more realistic images.

The generators G_A and G_B which we used are based on ResNet with 9 residual blocks and skip connections. Each block contains a convolutional layer, an instance normalization layer and a ReLU activation function. These blocks are connected with a few downsampling/upsampling operation. For the discriminators D_A and D_B, 7 convolutional blocks with each contains a convolutional layer, an instance normalization layer and a Leaky ReLU activation function are used. More details can be found in the original code[2].

As we can see from Figure 2, the generators G_A and G_B first learn the maps $G_A : \mathcal{B} \mapsto \mathcal{A}$ and $G_B : \mathcal{A} \mapsto \mathcal{B}$. The object of minimizing the adversarial loss

$$\mathcal{L}_{gan} = \mathbb{E}_A[\|1 - D_A(G_A(B))\|_2] + \mathbb{E}_B[\|1 - D_B(G_B(A))\|_2]. \tag{1}$$

To avoid tint change of the generated images, the CycleGAN introduces the identity loss to encourage the mapping to preserve color composition between the input and output. The identity loss regularizes the generator be closed to an identity mapping when real samples of the target domain are provided as the input to the generator. That is to minimize the loss

$$\mathcal{L}_{id} = \mathbb{E}_A[\|(G_A(A) - A)\|_1] + \mathbb{E}_B[\|(G_B(B) - B)\|_1]. \tag{2}$$

To further regularize the mapping function, the CycleGAN introduces the cycle-consistency loss. It enables that the generated image from one domain can translate back to its own domain. That is to say, the cycle-consistency loss enforces forward-backward consistency. The cycle-consistency loss can be defined as

$$\mathcal{L}_{cyc} = \mathbb{E}_A[\|(G_A(G_B(A)) - A)\|_1] + \mathbb{E}_B[\|(G_B(G_A(B)) - B)\|_1]. \tag{3}$$

In the end, the object of the generators is to minimize the loss

$$\mathcal{L}_G = \lambda_{gan}\mathcal{L}_{gan} + \lambda_{id}\mathcal{L}_{id} + \lambda_{cyc}\mathcal{L}_{cyc}. \tag{4}$$

After the images are generated from G_A and G_B, they will be provided as the input of the discriminators. The object of discriminators D_A and D_B is to identify the input image is the original images A and B or the images generated from G_A and G_B. Therefore the discriminators is trying to maximize the loss

$$\begin{aligned}\mathcal{L}_D = {} & \mathbb{E}_A[\|D_A(G_B(A))\|_2 + \|(D_A(A) - 1)\|_2] \\ & + \mathbb{E}_B[\|D_B(G_A(B))\|_2 + \|(D_B(A) - 1)\|_2].\end{aligned} \tag{5}$$

B. CycleGAN watermarking

In this section, a detail description of CycleGAN watermarking will be given. We adopt the strategy that the watermark decoder is pre-trained and frozen before training the CycleGAN watermarking. In the following, the way that we train watermark decoder and the CycleGAN watermarking will be introduced.

Watermark encoder-decoder: In CycleGAN watermarking, Alice and Bob can verify the host network through

[2]https://github.com/junyanz/pytorch-CycleGAN-and-pix2pix

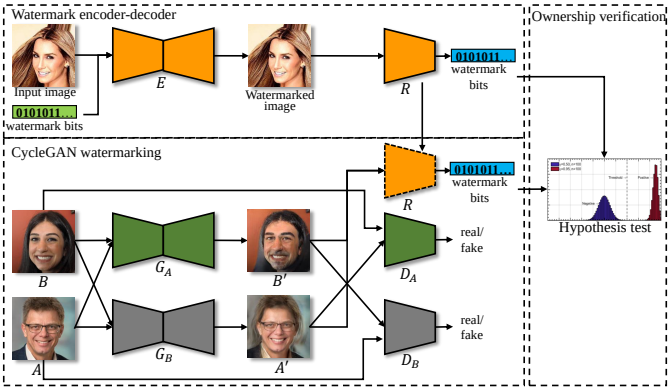

Fig. 2. The procedure of CycleGAN watermarking and ownership verification.

extracting the watermark from the output image. In our work we used the watermark encoder-decoder (StegaStamp) in [17] to learn how to extract the watermark. As shown in Figure 2, Bob trains a watermark encoder-decoder initially. The encoder E is trained to embed an arbitrary watermark bits into arbitrary images imperceptibly, while the decoder R is trained to extract that watermark bits w. The object of E is to learn a map from original image I to an image I_w with watermark, that is $E : (I, w) \mapsto I_w$, where $E(I, w) = I_w$ and it subjects to $I \approx I_w$. Simultaneously, the object of R is to reconstruct watermark bits $R : I_w \mapsto w$, where $R(I_w) = \hat{w}$ and it subjects to $w \approx \hat{w}$. They use mean square error (MSE) los function and binary cross entropy (BCE) loss function as the criterion to measure the distance between I and I_w, and the distance between w and $\hat{w}$ separately. In the end, the loss function of the watermark encoder-decoder is

$$\mathcal{L}_E = \mathbb{E}_I[\|(E(I, w), I)\|_2] + \lambda_e \mathbb{E}_I[\log(R(E(I, w)), w)], \quad (6)$$

where λ_e is a hyper-parameter to balance the two objective terms. After the watermark decoder R is training well, we freeze and use it to train the CycleGAN watermarking.

CycleGAN watermarking: The CycleGAN contains two generators and two discriminators, watermarking both the generators is meaningful since the application may release all the translation functions of the CycleGAN as APIs. Therefore, two n-bits watermark w_A and w_B are embedded when learning the maps $G_A : \mathcal{B} \mapsto \mathcal{A}$ and $G_B : \mathcal{A} \mapsto \mathcal{B}$. To embed w_A and w_B into CycleGAN, one can easily introduce the loss function for the adversarial input. As shown in Figure 3(a), the watermark maps are $R : G_A(\mathcal{B}) \mapsto w_A$ and $R : G_B(\mathcal{A}) \mapsto w_B$. Here only one watermark decoder R is needed since arbitrary watermark bits can be extracted from R [17]. In CycleGAN watermarking, the BCE loss is used measure the distance between w_A and $R(G_A(B))$, also for the distance between w_B and $R(G_B(A))$:

$$\mathcal{L}_{ganw} = \mathbb{E}_A[\log(R(G_B(A)), w_B)] + \mathbb{E}_B[\log(R(G_A(B)), w_A)]. \quad (7)$$

As we can see in Figure 3(b), the CycleGAN enables the translated image as close as the original input and thus has the cyclic maps $G_A : G_B(\mathcal{A}) \mapsto \mathcal{B}$ and $G_B : G_A(\mathcal{B}) \mapsto \mathcal{A}$. Suppose we already have the watermarked G_A and G_B with training the watermark loss (7), The cyclic maps without watermark will erase the embedded watermark when back propagating the watermark into the weights of G_A and G_B. To alleviate this effect, watermark loss for cyclic inputs must be added:

$$\begin{aligned}\mathcal{L}_{cycw} = &\mathbb{E}_A[\log(R(G_A(G_B(A))), w_A)] \\ &+ \mathbb{E}_B[\log(R(G_B(G_A(B))), w_B)].\end{aligned} \quad (8)$$

In fact, without introducing the watermark loss for cyclic inputs, one can see the binomial test in Figure 5 of the task man2woman for example, the bitwise accuracy is about 60%, which is far less than the requirements.

Similar to the cyclic watermark loss, we define the watermark loss function for identity inputs:

$$\mathcal{L}_{idw} = \mathbb{E}_A[\log(R(G_A(A)), w_A)] + \mathbb{E}_B[\log(R(G_B(B)), w_B)]. \quad (9)$$

Therefore the total generative loss for CycleGAN watermarking is

$$\mathcal{L}_{GW} = \lambda_{ganw}\mathcal{L}_{ganw} + \lambda_{idw}\mathcal{L}_{idw} + \lambda_{cycw}\mathcal{L}_{cycw}, \quad (10)$$

where λ_{ganw}, λ_{idw} and λ_{cycw} are the hyper-parameters that used to adjust the importance of the three watermark loss items. In the end, the object of CycleGAN watermarking is to minimize the loss

$$\mathcal{L} = \mathcal{L}_G + \mathcal{L}_{GW}. \quad (11)$$

C. Watermark verification

As we said in Section III, ownership verification is carried out by extracting the watermark from one image I (or more images) generated by the to-be-inspected network and check if the watermark corresponds to the watermark of the owner. Such a verification can be cast into a rigorous hypothesis testing problem as detailed below (see also [18]). Let $\hat{w}$ be the sequence of watermark bits extracted from the analyzed image, and let w be the watermark of the model's owner. Let n be the number of bits the watermark consists of, and let k be the number of matching bits between $\hat{w}$ and w. Watermark verification corresponds to running an hypothesis test between the null hypothesis H_0 that I does not contains w and the alternative hypothesis H_1 that I contains w, based on the observation of k. Under H_0, the bits in w and $\hat{w}$ are independent of each other and hence k follows a binomial distribution

$$\Pr(K = k) = \binom{n}{k}\eta^k(1-\eta)^{n-k}, \quad (12)$$

with $\eta = 0.5$. Under H_1, we can assume that the watermark bits are retrieved with an error probability p. By further assuming that bit errors are independent of each other, k still follows a binomial distribution with $\eta = 1 - p$. If p is not too large and n is large enough, the two hypothesis can be easily distinguished by comparing k against a detection threshold T to be set in such a way to find a good tradeoff between false positive and missed detection error probabilities.

The effectiveness of the test can be measured by looking at the ROC (Receiver Operating Characteristic) curve of the test

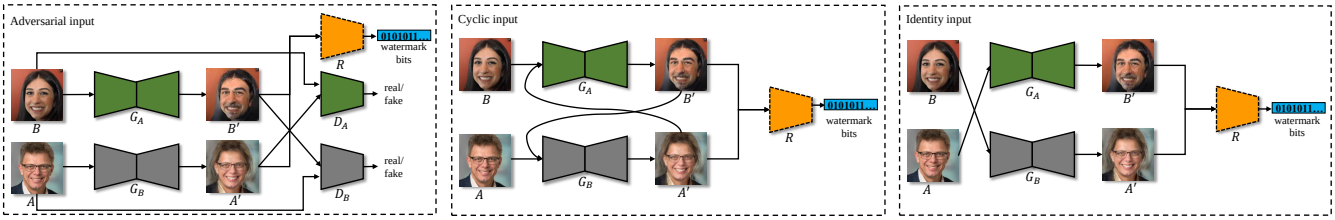

Fig. 3. The CycleGAN partial watermarking procedure for (a) adversarial input, (b) cyclic input and (c) identity input.

and the corresponding AUC (Area Under the Curve). Alternatively, we may consider the missed detection probability for a given false positive rate (FPR). In the following, we will adopt the latter approach and report the missed detection probability for a false alarm rate (FAR) equal to 1%. If the verification can be based on the observation of more images produced by the network[3], the effectiveness of the test improves. By assuming that the bit errors on different images are independent of each other, and by indicating with m the number of images involved by the test, the accuracy of the test is still ruled by Eq. (12), by replacing n with nm.

Here we take a successful verification in our experiments (see Figure 4) for example. We set $n = 200$ and obtain the average bitwise accuracy of 50.6% and 97.7% under hypothesis H_0 and H_1 is obtained, respectively. For the given FAR of 1%, the threshold can be settled as $T = 120$. In Figure 4, the AUC for $k \geq 120$ is

$$\begin{aligned} \Pr(k \geq 120|H_1) &= \sum_{k=120}^{200} \Pr(k|H_1) \\ &= 99.8\%, \end{aligned} \tag{13}$$

and missed detection probability is $1 - 99.8\% = 0.2\%$. It indicates the threshold is perfect to distinguish H_0 and H_1, and the number of matching bits is significantly enough for verification. On the contrary, as shown in Figure 5, the average bitwise accuracies are 50.6% and 58.62% under hypothesis H_0 and H_1, respectively. For the given FAR of 1%, the AUC for $K \geq 120$ is $\Pr(K \geq 120|H_1) = \sum_{k=120}^{200} \Pr(k) = 44.3\%$. and the missed detection probability is 55.7%, which indicates the result is far from enough for verification.

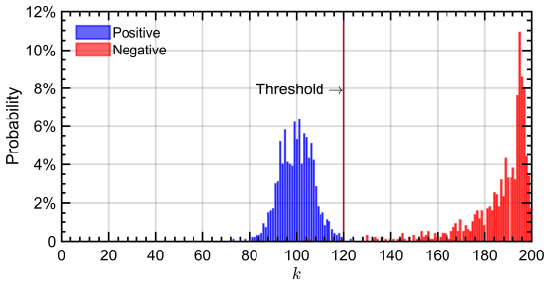

Fig. 4. Binomial probabilities density function for hypothesis test where the average bitwise accuracies are 50.6% (Negative) and 97.7% (Positive).

[3]This is the case, for instance, when the verifier can access the network under analysis through an API.

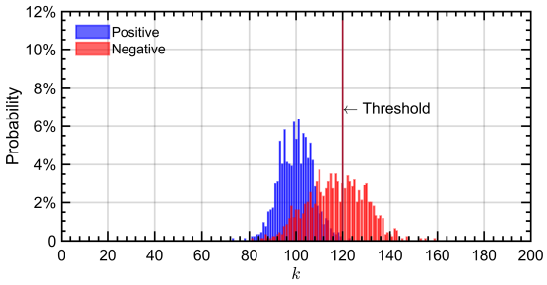

Fig. 5. Binomial probabilities density function for hypothesis test where the average bitwise accuracies are 50.6% (Negative) and 58.6% (Positive).

V. Experiments

In this section, a precise description about experimental results is given. We first give the watermark embedding evaluations in Section V-A. In Section V-B, we present the robustness analysis against image post-processing under a black-box access of the model. We give the ability of the model against surrogate model attack from malicious uses of the adversary in Section V-C. The ablation study for the watermark loss functions is given in Section V-D. The last Section describes the comparison results with different watermark embedding strategies.

A. Watermark embedding

Training: The dataset we used to train the watermark encoder-decoder described in Section IV-B is CelebA dataset [24], which contains 202,599 face images. The watermark encoder-decoder was trained for 50 epochs and the size of the input image was set to $256 \times 256 \times 3$. The Adam optimizer with learning rate of 0.0001 was used. The batch size was set to 64 and we took about 1 day to train the model on a GPU of NVIDIA-GeForce RTX 3070. The length of the watermark bits n was set to 200 bits. Detail about the code can refer to the original paper [17] and its code link.

For the dataset for training CycleGANWM, we trained on three tasks: *winter2summer, man2woman* and *monet2photo*. For winter2summer and monet2photo in the two domains, we separately used a maximize of 1,000 images for training. For man2woman, FFHQ dataset [25], which contains 70,000 high-quality PNG images at 1024×1024 resolution. We randomly chose 3,000 male images and 3,000 female images in FFHQ for training according to the gender label [26]. For the test of each tasks, we separately used a maximize of 1,000 images in each domains. The CycleGANWM was trained for 200 epochs

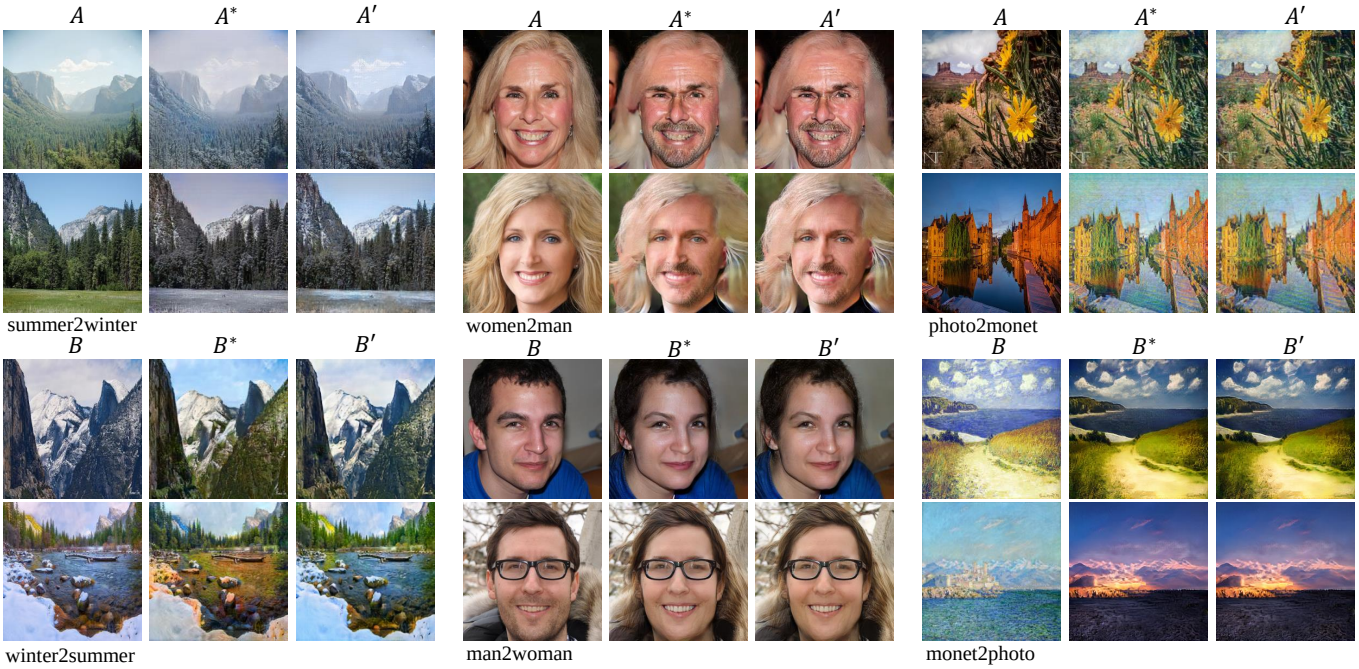

Fig. 6. The results for CycleGANWM for different tasks. In each task, the left is the original image, in the middle is the transferred image for non-watermarked CycleGAN, the right one is the output for watermarked CycleGAN.

and the size of the input image was set to $256 \times 256 \times 3$. For each network of the model, the Adam optimizer was used with β_1 set to 0.5, β_2 to 0.999 and the learning rate set to 0.0002. The batch size was fixed to 1. The weights for the CycleGAN loss function in Eq. (4) was set to $\lambda_{gan} = 1$, $\lambda_{id} = 5$ and $\lambda_{cyc} = 10$, and the weights for watermark loss function Eq. (11) was set to $\lambda_{ganw} = 1$, $\lambda_{idw} = 1$ and $\lambda_{cycw} = 0.5$. It took about 3 days training for each tasks on one GPU of Tesla P100.

The visual results for different tasks for CycleGANWM is shown in Figure 6. In each transfer direction, we compare the results of CycleGANWM to the results of non-watermarked CycleGAN (in which the results is marked with a $*$ on the upper right side). From the results we can see that the watermark dose not seriously affect the visual quality of the transferred images, which satisfied the requirement of *Invisibility*. We settle on a binary watermark bits with length of $n = 200$ bits as it provides a good compromise between image transferred quality and information transfer, and it leads to a larger enough watermark space for distinguishing a maximize number of 2^{200} models. Therefore it satisfies the requirement of *payload*.

We also evaluated the CycleGANWM for hypothesis test which introduced in Section IV-C. Here we report the results of the average bitwise accuracy (Avg bitacc) and missed detection probability (MDP) under the given FAR of 1% in Table I. It guarantees a very low missed detection probability, which means a good correct detection rate, for a sufficiently low FAR. Thus satisfies the requirement of *accuracy*.

TABLE I
THE AVERAGE BITWISE ACCURACY (AVG BITACC) AND THE MISSED DETECTION PROBABILITY (MDP) FOR CYCLEGANWM UNDER A FAR OF 1%.

Task	Avg bitacc	MDP
winter2summer	98.95	0
summer2winter	98.22	0
man2woman	98.46	0.10
woman2man	98.60	0
monet2photo	98.75	0
photo2monet	97.47	0.20

B. Robustness analysis

In this section, we discuss the robustness of the CycleGANWM against images post-processing. As we discussed in Section III, after CycleGANWM is trained well and deployed in the internet, the adversary (Eve) can only access the output image of CycleGANWM through an API with her own image as the input. Before verifying the ownership of the model, however, the output image may undergo image post-processing, and Eve may apply image processing on the output image for malicious usages and keep herself anonymous. In our experiments, we evaluated the robustness of the CycleGANWM against images post-processing of JPEG compression, adding Gaussian blur, adding Gaussian noise, brightness enhancement, contrast enhancement and saturation enhancement. Figure 7, 8 and 9 show the average bitwise accuracy of CycleGANWM for tasks of winter2summer, man2woman and monet2photo, respectively. For comparison, we also report the average bitwise accuracy of the watermark encoder-decoder (StegaStamp). For a given FAR of 1%, one can calculate and roughly set a threshold for the acceptable

TABLE II
THE ACCEPT RANGE FOR CYCLEGANWM UNDER A FAR OF 1%.

Task	Accept range (w/o data argumentation / with data argumentation)					
	JPEG compression	Gaussian blur	Gaussian noise	Brightness enhancement	Contrast enhancement	Saturation enhancement
winter2summer	100 / [100,80]	[1,9] / [1,15]	[0,0.4] / [0,0.4]	[0,0.8] / [0,2.0]	[0,1.6] / [0,2.0]	[0,2.0] / [0,2.0]
summer2winter	100 / [100,80]	[1,11] / [1,15]	[0,0.4] / [0,0.4]	[0,1.0] / [0,2.0]	[0,2.0] / [0,2.0]	[0,2.0] / [0,2.0]
man2woman	100 / [100,80]	[1,15] / [1,19]	[0,0.4] / [0,0.4]	[0,2.0] / [0,2.0]	[0,2.0] / [0,2.0]	[0,2.0] / [0,2.0]
woman2man	100 / [100,80]	[1,15] / [1,17]	[0,0.4] / [0,0.4]	[0,2.0] / [0,2.0]	[0,2.0] / [0,2.0]	[0,2.0] / [0,2.0]
monet2photo	100 / [100,80]	[1,17] / [1,19]	[0,0.4] / [0,0.4]	[0,1.4] / [0,2.0]	[0,2.0] / [0,2.0]	[0,2.0] / [0,2.0]
photo2monet	100 / [100,70]	[1,17] / [1,19]	[0,0.4] / [0,0.4]	[0,2.0] / [0,2.0]	[0,2.0] / [0,2.0]	[0,2.0] / [0,2.0]

bitwise accuracy is larger than 70% for all the tasks. Therefore, the accepting rage for each image post processing is shown in Table II.

In order to make the watermark embedding more robust against the image processing, we consider to add data argumentations after the image is transferred from CycleGANWM. This is similar as adding a noise layer [21] after the image is transferred, but adding data argumentation is more easy to train the CycleGANWM. By doing this the image after post processing can be seen in the training of CycleGANWM and thus make it robust against these image post processing. In our experiments, we randomly choose 50% images from the output images add the data argumentations which follow the settings in Table III, and then train the CycleGANWM with the enhanced output. Let CycleGANWM# be the model with data argumentation, we have the results of robustness analysis as shown in Figure 7, 8 and 9. The accept range is shown in Table II.

From Figure 7, 8, 9 and Table II we can observe that

1) When the quality factor of JPEG compression, the kernel size of Gaussian blur, the standard deviation of Gaussian noise, or the factor of color enhancements is increase, the average bitwise accuracy of the proposed CycleGANWM drops monotonously.
2) The proposed CycleGANWM is, to some extend, robust against Gaussian blur, Gaussian noise, brightness enhancement, contrast enhancement and saturation enhancement, but not robust against JPEG compression when the quality factor is less than 90.
3) A strong image post processing will degrade the watermark, and affect the accept range of verification for the ownership of the model.
4) With data argumentations, the robustness of the proposed CycleGANWM is improved against image post processing.
5) The accept range for the image post processing is larger enough for ownership verification.

Finally, the propose CycleGANWM satisfies the requirement of *robustness*.

C. Surrogate model attack

In real world scenario, Eve can do more things than image post processing. Although Eve can only access the model under a black-box way, which means only Eve can only access several output images from CycleGANWM through an API,

TABLE III
THE DATA ARGUMENTATIONS USED FOR CYCLEGANWM TRAINING.

Data argumentation	Range and interval
JPEG compression	[50:10:90]
Gaussian noise	[0:0.05:0.3]
Gaussian blur	[0:1:7]
Brightness enhancement	[0:0.2:1.2]
Contrast enhancement	[0:0.2:1.2]
Saturation enhancement	[0:0.2:1.2]

but does not know anything about the training parameters and dataset, the model's structure and the watermark. However, Eve still can use a different network structure trained with different loss functions to imitate CycleGAN's behavior, while erase the watermark from the output images. This is often referred to a surrogate model attack. Therefore, in this section, we formulate such a attack scenario and test the ability of CycleGANWM against this attack.

We supposed Eve uses pix2pix network [1] as the backbone network in the surrogate model. The UNet [27] and ResNet (the same as we used in CycleGANWM) were used as the generator for variation in pix2pix. The Adam optimizer was used with β_1 set to 0.5, β_2 to 0.999 and the learning rate set to 0.0002. To attack CycleGANWM on the task of winter2summer, we collected 4,000 and 1,000 landscape images from the internet to train and test the pix2pix network. For the task of man2woman, we randomly selected 3,000 and 1,000 face images from FFHQ for training and testing. For the task of monet2photo, we collected 2,756 painting images from the internet, in which 2,256 images was used for training, 500 images was used for testing. In Table IV, a detail number of the images used for training and testing the surrogate model is given, note that the landscape images are also used to train in monet2photo.

TABLE IV
THE TRAINING SETTINGS FOR THE SURROGATE MODEL ATTACK.

Task	dataset	Number of the images (train/test)
winter2summer	lanscape1	2,000/500
summer2winter	lanscape2	2,000/500
man2woman	FFHQ	3,000/500
woman2man	FFHQ	3,000/500
monet2photo	painting	2,256/500
photo2monet	lanscape1	2,000/500

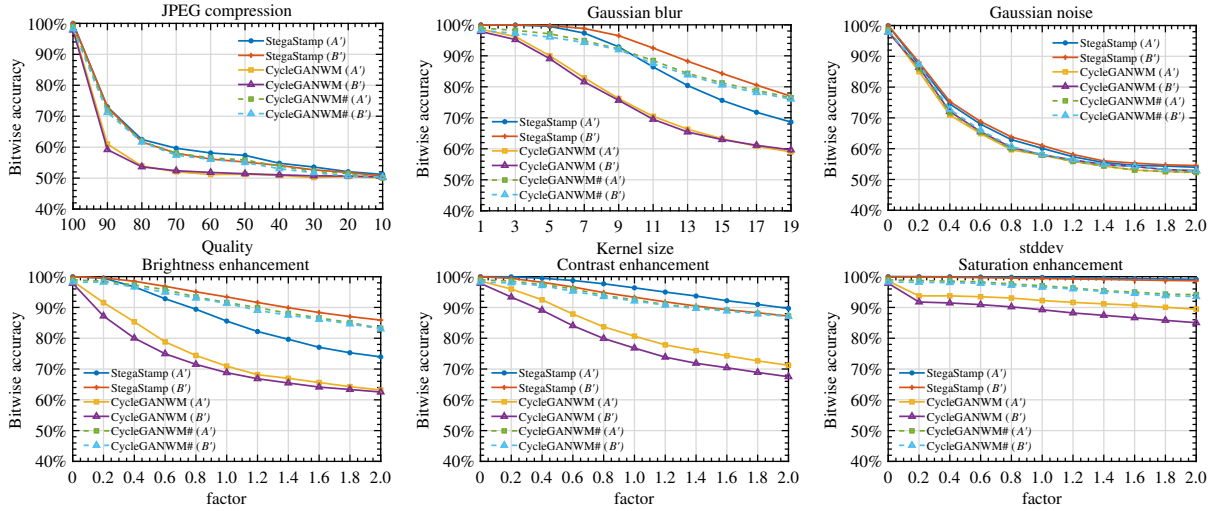

Fig. 7. The average bitwise accuracy for different models on task of winter2summer.

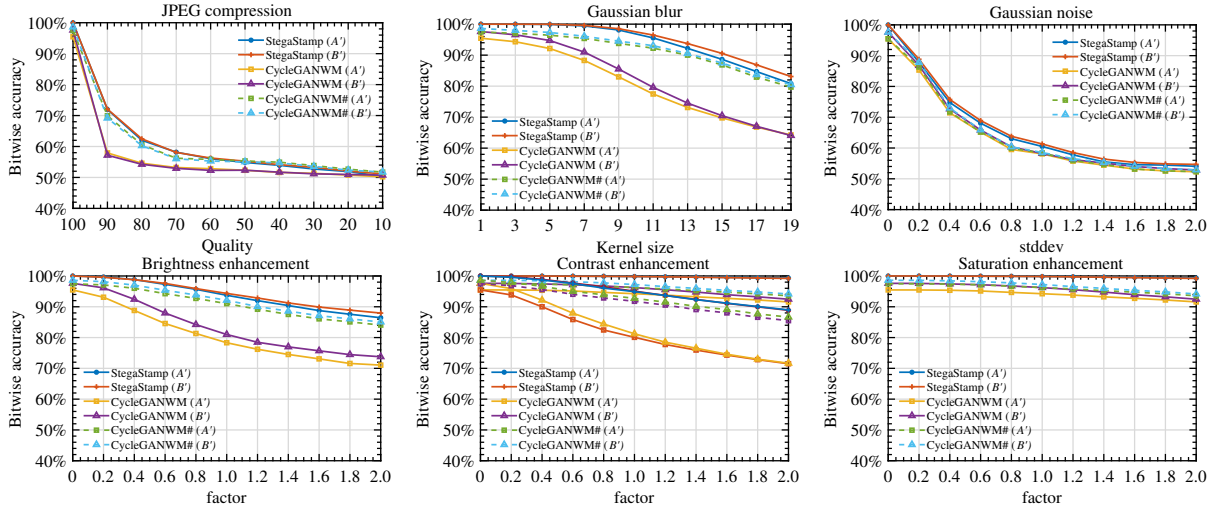

Fig. 8. The average bitwise accuracy for different models on task of man2woman.

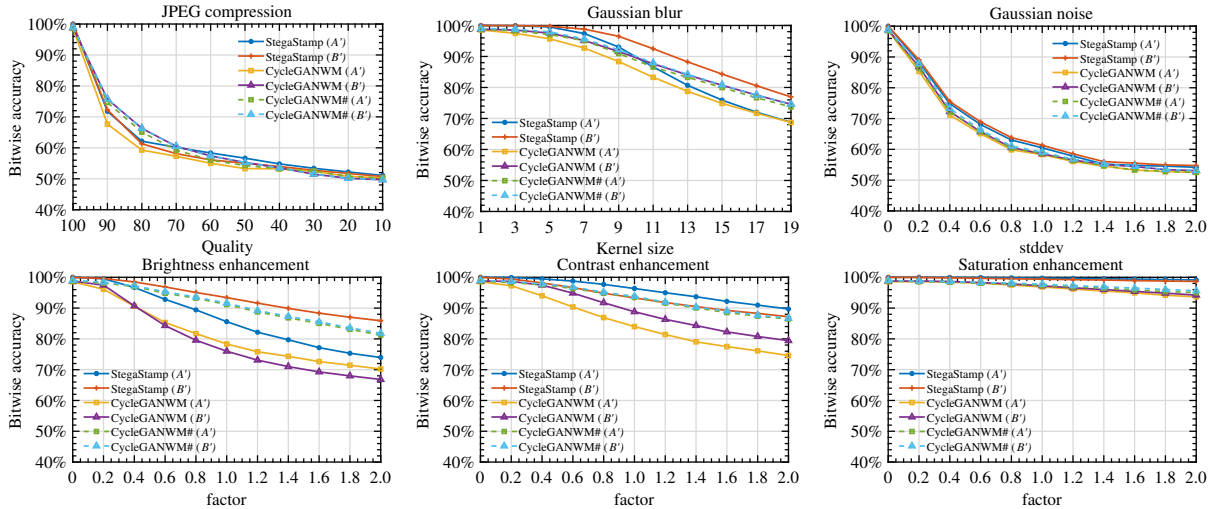

Fig. 9. The average bitwise accuracy for different models on task of monet2photo.

Once the training of the surrogate model is finished, Eve can use the generated images from the surrogate model to attack CycleGANWM. If the missed detection probability is too large, then the verification of CycleGANWM is failed. Therefore, as shown in Table V, we report the average bitwise accuracy (Avg bitacc) and the missed detection probability (MDP) for the generated images from the surrogate model. The FAR was settled as 1%, and the results for using ResNet and UNet as the generator in pix2pix were reported separately. From Table V we observe that the MDP is lower than the given FAR, which means the output images from the surrogate model still can be used to differentiate from a random guess model, even though the average bitwise accuracy is around 72%. In other words, the proposed CycleGANWM is robust against surrogate model attack.

TABLE V
THE AVERAGE BITWISE ACCURACY (AVG BITACC) AND THE MISSED DETECTION PROBABILITY (MDP) FOR SURROGATE MODEL ATTACK UNDER A FAR OF 1%.

Task	ResNet		UNet	
	Avg bitacc	MDP	Avg bitacc	MDP
winter2summer	75.59	0	71.00	0
summer2winter	76.01	0	71.27	0
man2woman	76.18	0.10	70.98	0.20
woman2man	76.34	0	71.59	0.20
monet2photo	77.93	0	72.45	0.20
photo2monet	72.77	0.20	70.23	0.40

D. Ablation study

In this section, the ablation study about the watermark loss functions of Eq. (7), (8) and (9) will be given. For the loss functions of Eq. (7) and (9), we can see that the inputs of G_A and G_B are the images A and B. If Bob wants to embed the watermark into the model and makes all the outputs of the generators contain watermark, he needs to calculate the losses for both Eq. (7) and (9). As for the loss function of Eq. (8), the inputs are the generated images from the generators, where they are represented as $G_A(B)$ and $G_B(A)$. These images are already watermarked and sent to another generator. As we discussed in Section IV-B, the cyclic input without watermark loss will erase the watermark from the output images. Through adjusting the weight λ_{cycw} in Eq. (11), the watermark will keep in the output images. Besides, the weights for $\mathcal{L}_{cycw}$ and $\mathcal{L}_{idw}$ should not be too large since different inputs for the discriminators (see Eq. (5)) will affect them when distinguishing the output images, thus casing a strong perturbation on the image content in adversarial training.

In our experiments, we considered three conditions

1) $\mathcal{L}_{ganw} = 0$, $\mathcal{L}_{cycw} = 0.5$ and $\mathcal{L}_{idw} = 1$,
2) $\mathcal{L}_{ganw} = 1$, $\mathcal{L}_{cycw} = 0$ and $\mathcal{L}_{idw} = 1$,
3) $\mathcal{L}_{ganw} = 1$, $\mathcal{L}_{cycw} = 0.5$ and $\mathcal{L}_{idw} = 0$,

using the method of control variates. Therefore we have obtained the average bitwise accuracy and missed detection probability of these variate models as Table VI shows. From this Table we observe that the missed detection probability is larger than the given FAR, which indicates the models trained without calculating even one watermark losses of Eq. (7), (8) and (9), will lead a failed verification of the ownership.

TABLE VI
THE AVERAGE BITWISE ACCURACY (AVG BITACC) AND THE MISSED DETECTION PROBABILITY (MDP) FOR ABLATION STUDY OF THE WATERMARK LOSS FUNCTIONS UNDER A FAR OF 1%.

Task	Condition 1)		Condition 2)		Condition 3)	
	Avg bitacc	MDP	Avg bitacc	MDP	Avg bitacc	MDP
winter2summer	62.45	32.80	60.35	50.70	65.60	1.20
summer2winter	59.00	44.40	58.32	55.70	62.23	30.40
man2woman	58.62	55.70	59.95	50.60	62.59	29.10
woman2man	58.34	55.70	60.17	49.40	62.35	30.20
monet2photo	61.27	37.80	60.28	50.50	63.38	15.70
photo2monet	60.34	50.60	59.95	51.20	62.05	31.00

E. Comparison

In our experiments, we also considered to compare the CycleGANWM to the existing GAN model watermarking embedding method which carries a binary watermark bits. The embedding strategies of [17] and [21] were considered for comparison. Because the method [17] and [21] did not watermark a CycleGAN, but their training strategy can be used for training CycleGANWM. Without loss the generality, we trained the CycleGANWM which follows the training scenarios of [17] and [21]. We describe the training strategies as follows.

- For the method [17], they adopt training the GAN models watermarked images which generated by the watermark encoder-decoder (StegaStamp). They trained the GAN models with original loss functions of the GAN models and without watermark loss functions. It means that we train CycleGANWM without calculating loss functions of Eq. (7), (8) and (9). In the mean time, we train CycleGANWM with watermarked images where the images are generated from the watermark encoder-decoder.
- For the method [21], they first train the GAN models, and then fine-tune the model with calculating the watermark loss function for several iterations. Therefore we also train CycleGAN initially, and then fine-tuning it for 2,000 iterations to embed watermark.

Then we compare model's performance of the proposed CycleGANWM with the models trained with the strategies from [17] and [21]. The missed average bitwise accuracy, detection accuracy and time complexity are considered as the performance metrics of these models. Table VII shows the results of average bitwise accuracy and missed detection probability of the models.

From the Table we can see that training with only watermarked images leads to a very high missed detection probability, therefore it does not work at all, while fine-tuning on a pretrined CycleGAN works for watermark embedding. However, the proposed CycleGANWM still has its strength on computing time complexity when the model is train from scratch. Actually, in our experiments, it took 6 more hours to fine-tune the CycleGAN with watermark loss functions for 2,000 iterations. More importantly, if we continue fine-tuning the CycleGANWM, the average bitwise accuracy drops

and ends to around 65% for 200 epochs of fine-tuning, while it will not happened for the proposed CycleGANWM (although at most cases such a long time fine-tuning will not be considered.).

TABLE VII
THE AVERAGE BITWISE ACCURACY (AVG BITACC) AND THE MISSED DETECTION PROBABILITY (MDP) FOR COMPARISON UNDER A FAR OF 1%.

Task	CycleGANWM		CycleGANWM with [17]		CycleGANWM with [21]	
	Avg bitacc	MDP	Avg bitacc	MDP	Avg bitacc	MDP
winter2summer	98.95	0	50.12	99.80	97.90	0
summer2winter	98.22	0	49.32	99.50	98.23	0
man2woman	98.46	0.10	50.10	99.80	98.12	0
woman2man	98.60	0	49.89	100	98.32	0
monet2photo	98.75	0	49.75	100	98.88	0.1
photo2monet	97.47	0.20	50.01	99.90	98.05	0

VI. CONCLUSION

Deep model IPR protection for GAN models has attracted increasing attention in recent years. The existing methods apply model watermarking to protect the GAN models, which considers embedding a binary message into the GAN models. We filled the gaps that the existing GAN watermarking methods cannot be applied on CycleGAN, and no one has considered a box-free method for CycleGAN watermarking. We carefully study the watermark loss functions for CycleGANWM and evaluate its robustness against image post processing and the ability of resisting surrogate model attack. We shew that the proposed CycleGANWM is sufficient and, furthermore, our future work can be applying the CycleGAN watermarking on a bunch of variants GAN structure which based on CycleGAN.

REFERENCES

[1] P. Isola, J.-Y. Zhu, T. Zhou, and A. A. Efros, "Image-to-image translation with conditional adversarial networks," *CVPR*, 2017.

[2] J.-Y. Zhu, T. Park, P. Isola, and A. A. Efros, "Unpaired image-to-image translation using cycle-consistent adversarial networks," in *Proceedings of the IEEE International Conference on Computer Vision (ICCV)*, Oct 2017.

[3] J. P. Cohen, M. Luck, and S. Honari, "Distribution matching losses can hallucinate features in medical image translation," in *Medical Image Computing and Computer Assisted Intervention – MICCAI 2018: 21st International Conference, Granada, Spain, September 16-20, 2018, Proceedings, Part I*. Berlin, Heidelberg: Springer-Verlag, 2018, p. 529–536. [Online]. Available: https://doi.org/10.1007/978-3-030-00928-1_60

[4] G. Bargshady, X. Zhou, P. D. Barua, R. Gururajan, Y. Li, and U. R. Acharya, "Application of cyclegan and transfer learning techniques for automated detection of covid-19 using x-ray images," *Pattern Recognition Letters*, vol. 153, pp. 67–74, 2022. [Online]. Available: https://www.sciencedirect.com/science/article/pii/S0167865521004128

[5] J. Lin, Y. Pang, Y. Xia, Z. Chen, and J. Luo, "Tuigan: Learning versatile image-to-image translation with two unpaired images," in *Computer Vision – ECCV 2020*. Cham: Springer International Publishing, 2020, pp. 18–35.

[6] Z. Yi, H. Zhang, P. Tan, and M. Gong, "Dualgan: Unsupervised dual learning for image-to-image translation," in *Proceedings of the IEEE international conference on computer vision*, 2017, pp. 2849–2857.

[7] T. Kim, M. Cha, H. Kim, J. K. Lee, and J. Kim, "Learning to discover cross-domain relations with generative adversarial networks," in *International conference on machine learning*. PMLR, 2017, pp. 1857–1865.

[8] X. Mao, Q. Li, H. Xie, R. Y. Lau, Z. Wang, and S. Paul Smolley, "Least squares generative adversarial networks," in *Proceedings of the IEEE international conference on computer vision*, 2017, pp. 2794–2802.

[9] M. Arjovsky, S. Chintala, and L. Bottou, "Wasserstein generative adversarial networks," in *International conference on machine learning*. PMLR, 2017, pp. 214–223.

[10] Z. Zheng, Y. Bin, X. Lu, Y. Wu, Y. Yang, and H. T. Shen, "Asynchronous generative adversarial network for asymmetric unpaired image-to-image translation," *IEEE Transactions on Multimedia*, 2022.

[11] Y. Choi, M. Choi, M. Kim, J.-W. Ha, S. Kim, and J. Choo, "Stargan: Unified generative adversarial networks for multi-domain image-to-image translation," in *Proceedings of the IEEE conference on computer vision and pattern recognition*, 2018, pp. 8789–8797.

[12] J. Kim, M. Kim, H. Kang, and K. Lee, "U-gat-it: Unsupervised generative attentional networks with adaptive layer-instance normalization for image-to-image translation," *arXiv preprint arXiv:1907.10830*, 2019.

[13] A. Gokaslan, V. Ramanujan, D. Ritchie, K. I. Kim, and J. Tompkin, "Improving shape deformation in unsupervised image-to-image translation," in *Proceedings of the European Conference on Computer Vision (ECCV)*, 2018, pp. 649–665.

[14] M.-Y. Liu, T. Breuel, and J. Kautz, "Unsupervised image-to-image translation networks," *Advances in neural information processing systems*, vol. 30, 2017.

[15] Y. Li, H. Wang, and M. Barni, "A survey of deep neural network watermarking techniques," *Neurocomputing*, vol. 461, pp. 171–193, 2021.

[16] D. S. Ong, C. S. Chan, K. W. Ng, L. Fan, and Q. Yang, "Protecting intellectual property of generative adversarial networks from ambiguity attacks," in *Proceedings of the IEEE/CVF Conference on Computer Vision and Pattern Recognition*, 2021, pp. 3630–3639.

[17] N. Yu, V. Skripniuk, S. Abdelnabi, and M. Fritz, "Artificial fingerprinting for generative models: Rooting deepfake attribution in training data," in *IEEE International Conference on Computer Vision (ICCV)*, 2021.

[18] V. Skripniuk, N. Yu, S. Abdelnabi, and M. Fritz, "Black-box watermarking for generative adversarial networks," *arXiv e-prints*, pp. arXiv–2007, 2020.

[19] M. Tancik, B. Mildenhall, and R. Ng, "Stegastamp: Invisible hyperlinks in physical photographs," in *Proceedings of The Ieee/cvf Conference on Computer Vision and Pattern Recognition*, 2020, pp. 2117–2126.

[20] N. Thakkar. (2020) An empirical study of gan watermarking. [Online]. Available: https://inst.eecs.berkeley.edu/~cs194-26/fa20/upload/files/projFinalProposed/cs194-26-aek/

[21] J. Fei, Z. Xia, B. Tondi, and M. Barni, "Supervised gan watermarking for intellectual property protection," *Arxiv Preprint Arxiv:2209.03466*, 2022.

[22] J. Zhang, D. Chen, J. Liao, W. Zhang, H. Feng, G. Hua, and N. Yu, "Deep model intellectual property protection via deep watermarking," *IEEE Transactions on Pattern Analysis and Machine Intelligence*, 2021.

[23] H. Wu, G. Liu, Y. Yao, and X. Zhang, "Watermarking neural networks with watermarked images," *IEEE Transactions on Circuits and Systems for Video Technology*, vol. 31, no. 7, pp. 2591–2601, 2021.

[24] Z. Liu, P. Luo, X. Wang, and X. Tang, "Deep learning face attributes in the wild," in *Proceedings of International Conference on Computer Vision (ICCV)*, December 2015.

[25] T. Karras, S. Laine, and T. Aila, "A style-based generator architecture for generative adversarial networks," in *Proceedings of The Ieee/cvf Conference on Computer Vision and Pattern Recognition*, 2019, pp. 4401–4410.

[26] NVIDIA-DCGM, "Gender, Age, and Emotions extracted for Flickr-Faces-HQ Dataset (FFHQ)," https://github.com/DCGM/ffhq-features-dataset, 2020.

[27] O. Ronneberger, P. Fischer, and T. Brox, "U-net: Convolutional networks for biomedical image segmentation," in *International Conference on Medical image computing and computer-assisted intervention*. Springer, 2015, pp. 234–241.